AIP | Journal of Applied Physics

Investigating the impact of source/drain doping dependent effective masses on the transport characteristics of ballistic Si-nanowire field-effect-transistors

Basudev Nag Chowdhury and Sanatan Chattopadhyay

Citation: Journal of Applied Physics **115**, 124502 (2014); doi: 10.1063/1.4869495
View online: http://dx.doi.org/10.1063/1.4869495
View Table of Contents: http://scitation.aip.org/content/aip/journal/jap/115/12?ver=pdfcov
Published by the AIP Publishing

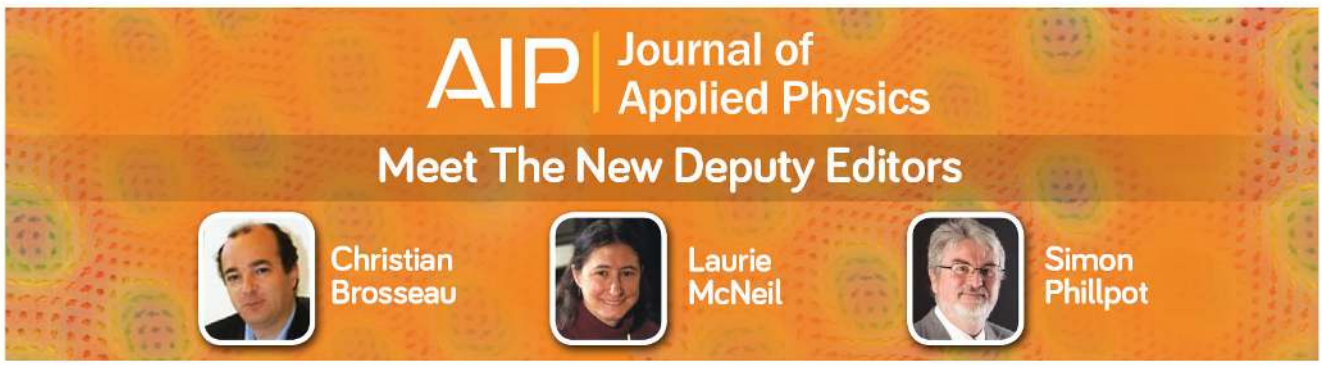

Investigating the impact of source/drain doping dependent effective masses on the transport characteristics of ballistic Si-nanowire field-effect-transistors

Basudev Nag Chowdhury[1] and Sanatan Chattopadhyay[2,a)]
[1]Centre for Research in Nanoscience and Nanotechnology (CRNN), University of Calcutta, Kolkata, India
[2]Department of Electronic Science, University of Calcutta, Kolkata, India

(Received 24 January 2014; accepted 11 March 2014; published online 26 March 2014)

This article studies the impact of doping dependent carrier effective masses of the source/drain regions on transport properties of Si-nanowire field effect transistors within ballistic limit. The difference of carrier effective mass in channel and that in the source/drain regions leads to a misalignment of respective sub-bands and forms non-ideal contacts. Such non-idealities are incorporated by modifying the relevant self-energies which control the effective electronic transport from source to drain through the channel. Non-ideality also arises in the nature of local density of states in the channel due to sub-band misalignment, resulting to a reduction of drain current by almost 50%. The highest values of drain current, leakage current, and their ratio are obtained for the S/D doping concentrations of 3×10^{20} cm^{-3}, 8×10^{20} cm^{-3}, and 2×10^{20} cm^{-3}, respectively, for the nanowire of length 10 nm and diameter of 3 nm. Interestingly, the maximum of sub-threshold swing, minimum of threshold voltage, and the maximum of leakage current are observed to be apparent at the same doping concentration. © *2014 AIP Publishing LLC*. [http://dx.doi.org/10.1063/1.4869495]

I. INTRODUCTION

The sustained evolution of metal-oxide-semiconductor field-effect-transistors (MOSFETs) following gradual downscaling of physical dimensions has led to the emergence of Silicon-nanowire field effect transistors (Si-NWFETs) for future nanoelectronic circuits.[1] In this regard, there has been a significant progress in realizing such nanowire based field effect devices and their fabrication has been performed by adopting both top-down and the bottom-up approaches.[2–11] In course of such aggressive downscaling, the device dimensions have entered into the ballistic regime that indicates carrier transport without any significant scattering.[12–14] For comprehensive understanding of the transport behavior of such devices, it is essential to develop quantum mechanical models which can incorporate the effects of discontinuities in the energy continuum and consequently the variation of the relevant effective mass components. Such a model can be obtained by developing a Schrodinger-Poisson simultaneous solver which is capable of simulating the quantum transport of charges. In this context, the non-equilibrium Green's function (NEGF) formalism has appeared as one of the most potential tools that can solve the quantum transport equations of electron in the MOSFET-channel, considering its interaction with source/drain (S/D) regions.[15] Several reports are available where such technique has been used to study the transport behavior of different nano-scale MOSFET architectures such as double gate MOSFET, FinFET, multiple-gate NWFET, gate-all-around (GAA) NWFET, nanotube FET, and molecular switch junctions.[16–24]

The physical behavior and quantification of charge transport from source to drain can be modeled by calculating the associated self energy of S/D regions. Self energy represents the interaction of the channel with S/D and it is estimated by assuming the S/D regions to be semi-infinite and hence the corresponding Hamiltonians are taken to be uniform.[15,25,26] However, the transport effective masses of the channel and S/D regions are not identical due to difference in their doping concentrations[27] and hence it modifies their interactions, leading to the change of transport behavior and electrical characteristics of the device. Therefore, the S/D doping concentrations play a significant role in designing such nanowire based FET devices. Consequently, the NEGF model given in Ref. 15 should be modified to incorporate such effects and a systematic study is crucial for developing a comprehensive understanding of the impact of doping dependent effective masses of the S/D regions.[28]

In the current article, the effect of variation of transport effective mass with doping concentration of the S/D regions has been incorporated into NEGF model through relevant modification of the self energy matrices. An abrupt change in transport mass is considered at the junctions of the channel and S/D regions, and the form of self energies is altered accordingly. The corresponding transport behavior of the carriers is analyzed in detail. To focus only on the impact of doping dependent effective masses of S/D, the electron phonon scattering has not been considered. Finally, the impact of S/D doping concentration on the electrical characteristics of Si-NWFETs is studied to explore its impact on the device performance.

II. THEORETICAL MODELING

Transport of the electrons from n^+-source to n^+-drain through a GAA intrinsic Si-nanowire channel is modeled by solving the simultaneous Schrödinger-Poisson equation given by

$$\hat{H}_{3D}|\psi\rangle = E|\psi\rangle \tag{1}$$

and

$$\vec{\nabla} \cdot \left(\varepsilon \vec{\nabla} \varphi\right) = -(-e) n_{3D}, \tag{2}$$

a)Email: scelc@caluniv.ac.in

where ε represents the permittivity of the entire device which varies at the material junctions, n_{3D} is 3-dimensional carrier concentration and $-e$ is the electronic charge. The 3-dimensional Hamiltonian ($\hat{H}_{3D}$) in the non-equilibrium state $|\psi\rangle$ is given by

$$\hat{H}_{3D} = \frac{1}{2}\sum_{j,k} \hat{p}_j (m*^{-1})^{jk} \hat{p}_k + (-e)\varphi, \tag{3}$$

where $\hat{\vec{p}}$ is the momentum operator, m^* represents the effective mass tensor, and φ is the potential of the bottom of conduction band. Gate length of the device is considered to be smaller than the electron mean free path so as to model the ballistic transport. Thus, the effect of scattering is not considered in the current work. The electrons are confined in the transverse direction due to GAA structure of the device thereby leading to the formation of discrete transverse energy sub-bands, which can be obtained from solutions of the equation,

$$\hat{H}_T|\chi\rangle_n = E_n^{sub}|\chi\rangle_n, \tag{4}$$

where $\hat{H}_T$ is the transverse part of the 3-D Hamiltonian. The non-equilibrium state ($|\psi\rangle$) for the 3-D motion of electrons can then be represented by superposition of the transverse eigenstates ($|\chi\rangle_n$) as

$$|\psi\rangle = \sum_n C_n|\chi\rangle_n, \tag{5}$$

which, in turn, gives rise to the matrix equation

$$\underline{\underline{H}}_L \underline{C} = \left(E\underline{\underline{I}} - \underline{\underline{E}}^{sub}\right)\underline{C}. \tag{6}$$

The block elements of longitudinal Hamiltonian matrix ($\underline{\underline{H}}_L$) are formed according to the sub-band states. The diagonal blocks represent the corresponding mode of transport and the off-diagonal blocks estimate the effect of inter-sub-band transitions. The elements of each block of $\underline{\underline{H}}_L$ are obtained using finite difference method (FDM) of 1st order by dividing the nanowire channel into grids with spacing "a." The blocks are, thus, tri-diagonal matrices, with diagonal elements representing the longitudinal transport energy and the others stand for the interactions (β) between the neighbouring grid points. Coupling of the nanowire channel with source and drain are incorporated by adding the corresponding self energies ($\sum_{\underline{\underline{S}}}$ and $\sum_{\underline{\underline{D}}}$) to the Hamiltonian by considering the interaction of the channel with S/D in the channel Green's function as[15]

$$\underline{\underline{G}} = \left(E\underline{\underline{I}} - \underline{\underline{E}}^{sub} - \left(\underline{\underline{H}}_L + \underline{\underline{\Sigma}}_S + \underline{\underline{\Sigma}}_D\right)\right)^{-1}. \tag{7}$$

The self energy matrices of source and drain have only non-zero elements at the 1st and last grid points, respectively, indicating their interaction only with the grid points at the S/D junctions. The elements have been found to be of the form "$\beta g \beta$,"[15,25,26] β being the grid interaction in the channel region and "g" is the solution of the equation,

$$(g)^{-1} = [E - E_n^{sub} + 2\beta_{S/D}] - \left(-\beta_{S/D}\right) g \left(-\beta_{S/D}\right). \tag{8}$$

Equation (8) is obtained by considering the S/D regions to be semi-infinite and the corresponding Hamiltonians to be entirely uniform.[25,26] The vicinity of the channel drain junction in the Green's function is represented by

$$\underline{\underline{G}}_n = \left[\begin{array}{cccc|ccccc} \ldots & \ldots & \ldots & \ldots & \ldots & \ldots & \ldots & \ldots & \ldots \\ \ldots & -\beta & [E - E_n((N-1)a) + 2\beta] & -\beta & 0 & 0 & 0 & 0 & \ldots \\ \ldots & 0 & -\beta & [E - E_n(Na) + 2\beta] & -\beta & 0 & 0 & 0 & \ldots \\ \hline \ldots & 0 & 0 & -\beta & [E - E_n^D + 2\beta_D] & -\beta_D & 0 & 0 & \ldots \\ \ldots & 0 & 0 & 0 & -\beta_D & [E - E_n^D + 2\beta_D] & -\beta_D & 0 & \ldots \\ \ldots & 0 & 0 & 0 & 0 & -\beta_D & [E - E_n^D + 2\beta_D] & -\beta_D & \ldots \\ \ldots & \ldots & \ldots & \ldots & \ldots & \ldots & \ldots & \ldots & \ldots \end{array}\right]^{-1}. \tag{9}$$

However, considering the change in local band structure at the channel-drain junction, the Green's function is modified by

$$\underline{\underline{G}}_n = \left[\begin{array}{cccc|ccccc} \ldots & \ldots & \ldots & \ldots & \ldots & \ldots & \ldots & \ldots & \ldots \\ \ldots & -\beta & [E - E_n((N-1)a) + 2\beta] & -\beta & 0 & 0 & 0 & 0 & \ldots \\ \ldots & 0 & -\beta & [E - E_n(Na) + 2\beta] & -\beta & 0 & 0 & 0 & \ldots \\ \hline \ldots & 0 & 0 & -\beta & [E - E_n^D + 2\bar{\beta}] & -\beta_D & 0 & 0 & \ldots \\ \hline \ldots & 0 & 0 & 0 & -\beta_D & [E - E_n^D + 2\beta_D] & -\beta_D & 0 & \ldots \\ \ldots & 0 & 0 & 0 & 0 & -\beta_D & [E - E_n^D + 2\beta_D] & -\beta_D & \ldots \\ \ldots & \ldots & \ldots & \ldots & \ldots & \ldots & \ldots & \ldots & \ldots \end{array}\right]^{-1} \tag{9A}$$

resulting in the modification of the elements of self energy matrices from "$\beta g \beta$" to "$(\frac{1}{1-2(\beta_{S/D}-\bar{\beta})g})\beta g \beta$," strength of the interaction being "$(\frac{1}{1-2(\beta_{S/D}-\bar{\beta})g})$." The grid interaction at the junction ($\bar{\beta}$) becomes simple arithmetic mean of that of the channel (β) and S/D ($\beta_{S/D}$) on considering a jump discontinuity in the local band structure at the channel-S/D junction leading to an abrupt change in the transport effective mass.

The local density of states in the channel due to coupling with source and drain corresponding to the n^{th} sub-band are given by[15]

$$\underline{\underline{D}}_S^n = \frac{1}{2\pi a}\left[\underline{\underline{G}}^n \underline{\underline{\Gamma}}_S \underline{\underline{G}}^{n^+}\right] \tag{10A}$$

and

$$\underline{\underline{D}}_D^n = \frac{1}{2\pi a}\left[\underline{\underline{G}}^n \underline{\underline{\Gamma}}_D \underline{\underline{G}}^{n^+}\right], \tag{10B}$$

where $\underline{\underline{\Gamma}}_S = i(\underline{\underline{\sum}}_S - \underline{\underline{\sum}}_S{}^+)$ and $\underline{\underline{\Gamma}}_D = i(\underline{\underline{\sum}}_D - \underline{\underline{\sum}}_D{}^+)$ represent the electron exchange rates between the channel and source/ drain contacts respectively, which gives rise to the 1-D carrier concentration as

$$n_{1D}^n = \int \left[D_S^n(z) f(E - E_{fS}) + D_D^n(z) f(E - E_{fD})\right] dE, \tag{11}$$

where $f(E - E_{fS})$ and $f(E - E_{fD})$ are the Fermi-Dirac distribution functions at source and drain contacts, respectively. The total 3-D carrier concentration is then given by

$$n_{3D} = \sum_n n_{1D}^n |\langle \vec{r}|\chi\rangle_n|^2. \tag{12}$$

The expression of (12) is applied into the Poisson's equation given in (2). The potential obtained from the solution of Eq. (2) is then put into Eq. (3) and the same process is continued until self-consistency is achieved. Finally, the drain current is obtained from Landauer formula,

$$I = \frac{2e}{h}\int T_{S\to D}(E)\big(f(E - E_{fS}) - f(E - E_{fD})\big) dE, \tag{13}$$

where $T_{S\to D}$ is the transmission coefficient given by[15]

$$T_{S\to D} = Trace[\Gamma_S G \Gamma_D G^+]. \tag{14}$$

III. RESULTS AND DISCUSSION

The structure of a cylindrical GAA Si-NWFET considered in the current model is schematically shown in Fig. 1(a) and the impact of source/drain doping concentration on the performance of such device is studied in detail. Diameter and channel length of the nanowire are considered to be 3 nm and 10 nm, respectively. The channel is considered to be along [100] direction which is one of the principal axes of Si. Thus the off-diagonal elements of the electron effective mass tensor become zero. The diagonal components of the effective mass in the Si nanowire channel are taken from Ref. 29, whereas, the values of the transport effective mass components in source and drain as a function of doping concentration are summarized in Table I.[27] Thickness of the SiO_2 layer all-around the channel is considered to be 1 nm. The doping concentration of source and drain is varied in the order of 10^{20}–10^{21} cm^{-3} and the doping of surrounded poly-Si gate is adjusted to obtain a zero (0 V) flat band voltage by assuming the identical Fermi energy in both the source and gate. The device is assumed to operate at room temperature (300 K).

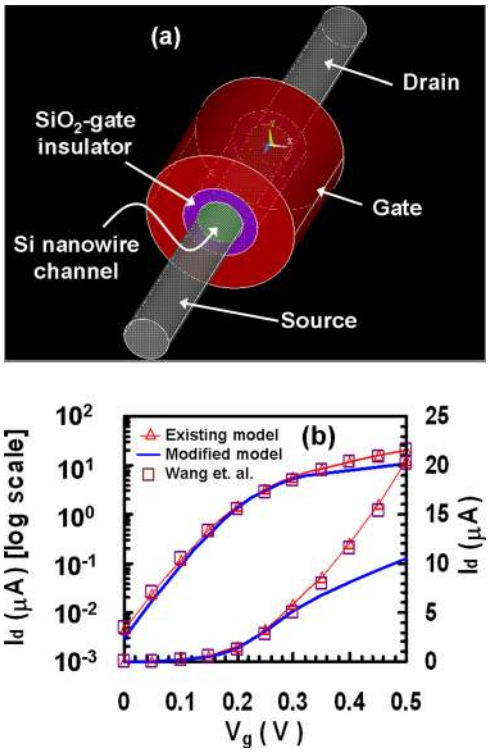

FIG. 1. (a) Schematic of a GAA Si-NWFET; (b) Comparison of transfer characteristics of the Si-NWFET for the modified model and the existing model calibrated with.[21]

TABLE I. Summary of transport effective mass of electron in Si with doping concentration.[27]

Doping concentration (10^{20}/cc)	Transport effective mass (m_e)
0.7	0.285
0.8	0.285
0.9	0.285
1	0.291
2	0.292
3	0.300
4	0.309
5	0.321
6	0.330
7	0.343
8	0.366
9	0.373
10	0.388

Transfer characteristics of the GAA Si-NWFET obtained from the current model with modified S/D self energy matrices, are plotted in Fig. 1(b). The results are also calculated from the existing model of Ref. 15 and then compared along with the data of Ref. 21, for the device with identical specifications and biases. It is apparent from Fig. 1(b) that the data obtained from our NEGF based Schrödinger-Poisson simultaneous solver matches quite satisfactorily with the published data of Ref. 21 thereby indicating the calibration and accuracy of the solver. However, it is interesting to note that the same solver gives rise to significant modification to the transfer characteristics of the device when the doping dependent transport effective mass of S/D is incorporated. It can be seen from the plot of Fig. 1(b) that the drain current may be reduced by 50% at a gate voltage of 0.5 V due to the effects of doping dependent effective mass of S/D regions.

The color plots of Figs. 2(a) and 2(b) compare the variation of local density of states (LDOS) with energy along the channel obtained from the existing and the current model (with modified self-energies), respectively. The corresponding values of LDOS at the centre of the channel and the relevant transmission coefficient are also depicted in Figs. 2(a) and 2(b). LDOS at any point in the nanowire channel depends on the strength of interaction of the point with S/D regions. For weak interaction, the LDOS curve shows sharp peaks (Fig. 2(b)) at the sub-bands whereas strong interaction leads to broadening of the levels (Fig. 2(a)). If the change in transport effective mass due to S/D doping is neglected in modeling the transport of NWFETs then the strength of interaction will be maximum, indicating an ideal contact. However, real systems pose severe challenges to attain an ideal ohmic contact at such nano-dimensions both from the technological as well as physical perspectives. This is due to the fact that the mismatch of transport effective masses between the channel and S/D regions creates a misalignment of sub-bands leading to a relatively weaker coupling. Therefore, the self-energy needs to be modified to realize a real contact for incorporating the effects of physical interactions between the channel and S/D regions. The transmission curve shows steps at the sub-bands for ideal ohmic contacts whereas for the non-ideal contacts it exhibits several maxima at the sub-bands. The maxima indicate a resonance of carrier transmission for higher degree of confinement in the channel due to lower transport effective mass in it compared to S/D regions. As a result, the area under the transmission curve for non-ideal contact turns out to be smaller than the ideal one leading to a reduction of drive current (Fig. 1(b)). It should be noted that the phonon scattering in such devices leads to broadening of levels thereby indicating an increase of area under the transmission curves. However, there will also be a reduction in the value of transmission coefficient and consequently, the net current will be reduced.[31,32]

Fig. 3 compares the one-dimensional carrier concentration and the conduction band profile along the channel for ideal and non-ideal contacts. It can be seen from the plots that the carrier concentration obtained from modified model is decreased by almost an order from the existing formalism near the source/channel and channel/drain junctions, however, it remains almost unaltered at central region of the channel. This is attributed to the reduced carrier probability near the channel-S/D junctions due to higher degree of local confinement. The conduction band profile shows that the barrier is lowered as a result of incorporating the effect of higher transport effective mass of electrons in the S/D regions. It should be noted that the barrier in a conventional MOSFET is only a function of doping concentrations of source, channel and drain since it originates from the electrostatic interaction of these regions. However, the carrier transport in quantum devices within ballistic regime is also guided by the uncertainty principle where the transport effective mass plays a significant role in forming the barrier. Relatively lower transport effective mass within the channel

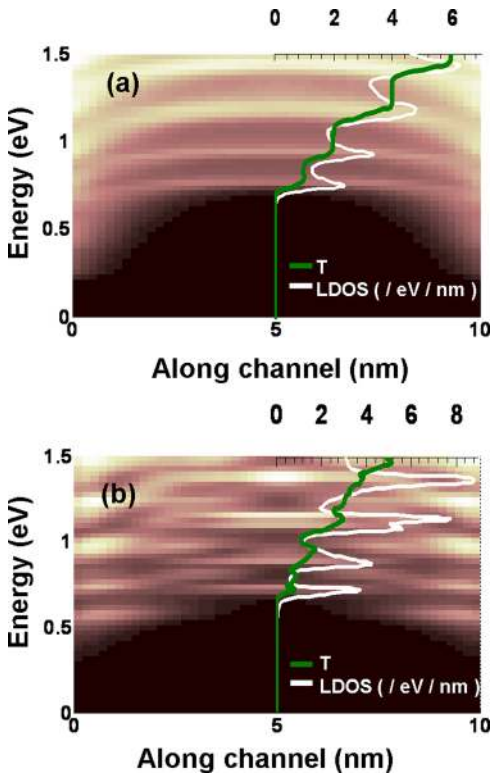

FIG. 2. Comparison between the ideal and non-ideal contacts: (a) plot of local density of states (LDOS) with energy along the channel, and the variation of LDOS at the centre of channel and transmission coefficient (T) vs. energy, obtained from the existing model; (b) same as (a), obtained from the modified model.

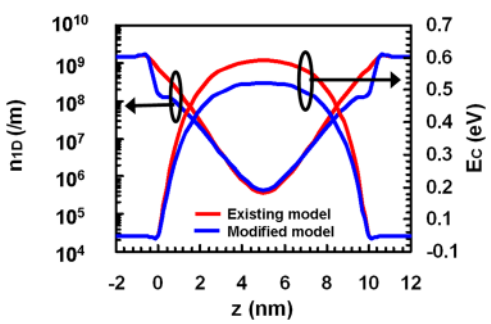

FIG. 3. Profile of the one dimensional carrier density and conduction band along the nanowire channel, obtained from the existing model and the modified model for ideal and non-ideal contacts, respectively.

compared to the S/D regions indicates higher uncertainty, resulting in lowering of barrier, as shown in Fig. 3.

The source/drain doping concentration of the device is varied in the range of 10^{20}–$10^{21}\,cm^{-3}$ and its performance parameters in terms of drive current, leakage current, their ratio, threshold voltage, and sub-threshold swing have been studied. Fig. 4(a) shows the bar plots of drive current (I_{on}), leakage current (I_{off}) and their ratio (I_{on}/I_{off}) as a function of source/drain doping concentration whereas Fig. 4(b) represents the bar diagram of threshold voltage (V_{th}) and sub-threshold swing (SS). It is observed from Fig. 4(a) that I_{on} increases initially at a faster rate up to a doping concentration of $3 \times 10^{20}\,cm^{-3}$ and then it almost saturates. However, the leakage current increases with doping and attains a maximum value of ~10 nA at the doping concentration of $8 \times 10^{20}\,cm^{-3}$. As a result, the I_{on}/I_{off} achieves a maximum value at a doping level of $2 \times 10^{20}\,cm^{-3}$. It is seen from the plots of Fig. 4(b) that the minimum of V_{th} and maximum of SS occur exactly at the doping level where I_{off} attains its maximum. Here, the threshold voltage has been considered at $I_D = 10$ nA and $V_D = 0.4$ V.[21] Hence, it is apparent that the threshold voltage required to turn the device "on" has an almost inverse correlation with the "off-current." However, SS is directly correlated to the channel carrier concentration in the sub-threshold region[30] and therefore with the "off-current." It should be noted that the S/D doping concentration and associated transport effective masses are the key parameters to control the performance metrics considered in the current work. The increase of doping concentration raises the Fermi levels of S/D regions leading to higher probability of coupling between the channel and S/D. Conversely, the larger transport effective mass of electrons in the S/D regions reduces such coupling. Therefore, the two key parameters are affecting the current values as well as the corresponding required voltages oppositely and the doping values at extremum are set by their relative dominance. Thus, the source/drain doping concentration is emerging to be a crucial parameter for designing high performance Si NWFETs.

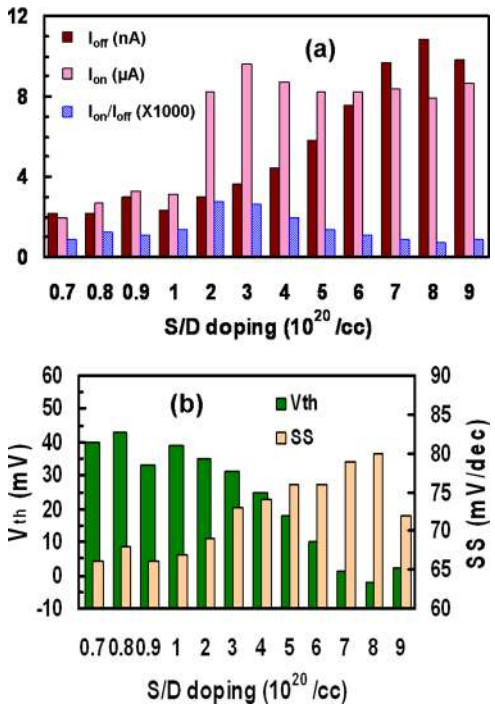

FIG. 4. (a) Bar plot of the drive-current, leakage-current, and the ratio of drive current to leakage current with source/drain doping concentration; (b) Bar plot of threshold voltage and sub-threshold swing with source/drain doping concentration.

IV. CONCLUSIONS

The effects of source/drain doping concentration on the ballistic transport characteristics of Si-nanowire field-effect-transistors (Si-NWFETs) have been studied in detail by considering the doping dependent effective mass of the carriers and the relevant modification of the self-energy matrices for S/D interaction with the channel. It is observed that the LDOS values in the channel depend strongly on the interaction of it with the S/D regions and the sub-bands are sharpened due to non-idealities of the contacts. The modification of self-energies by incorporating the doping dependent effective masses, drain current has been observed to be reduced by almost 50%. The highest values of drive current, leakage current, and their ratio are obtained at the S/D doping concentration of $3 \times 10^{20}\,cm^{-3}$, $8 \times 10^{20}\,cm^{-3}$, and $2 \times 10^{20}\,cm^{-3}$, respectively, for the current specification of the device. Interestingly, the maximum of SS and minimum of V_{th} occur at the same value as for the maximum of leakage current.

ACKNOWLEDGMENTS

The authors would like to acknowledge the University Grant Commission (UGC), Government of India, for funding the fellowship of Mr. Basudev Nag Chowdhury through the University of Calcutta.

[1]H. Iwai, Microelectron. Eng. **86**, 1520 (2009).
[2]Y. Shan, A. K. Kalkan, C. Y. Peng, and S. J. Fonash, Nano Lett. **4**, 2085 (2004).
[3]Y. Wang, V. Schmidt, S. Senz, and U. G. Sele, Nature Nanotechnol. **1**, 186 (2006).
[4]W. Lu and C. M. Lieber, Nature Mater. **6**, 841 (2007).
[5]D. Wang, B. A. Sheriff, M. McAlpine, and J. R. Heath, Nano Res. **1**, 9 (2008).
[6]G. Pennelli, Microelectron. Eng. **86**, 2139 (2009).
[7]H. D. Tong, S. Chen, W. G. van der Wiel, E. T. Carlen, and A. van den Berg, Nano Lett. **9**, 1015 (2009).
[8]H. Wang, M. Sun, K. Ding, M. T. Hill, and C. Z. Ning, Nano Lett. **11**, 1646 (2011).
[9]M. H. Ben-Jamaa, P. E. Gaillardon, F. Clermidy, I. O'Connor, D. Sacchetto, G. De Micheli, and Y. Leblebici, Sci. Adv. Mater. **3**, 466 (2011).
[10]R. G. Hobbs, N. Petkov, and J. D. Holmes, Chem. Mater. **24**, 1975 (2012).
[11]S. Jana, S. Mondal, and S. R. Bhattacharyya, J. Nanosci. Nanotechnol. **13**, 3983 (2013).
[12]S. Eminente, D. Esseni, P. Palestri, C. Fiegna, L. Selmi, and E. Sangiorgi, IEEE Trans. Electron. Devices **52**, 2736 (2005).
[13]K. H. Cho, K. H. Yeo, Y. Y. Yeoh, S. D. Suk, M. Li, J. M. Lee, M.-S. Kim, D. W. Kim, D. Park, B. H. Hong, Y. C. Jung, and S. W. Hwang, Appl. Phys. Lett. **92**, 052102 (2008).
[14]R. Wang, H. Liu, R. Huang, J. Zhuge, L. Zhang, D. W. Kim, X. Zhang, D. Park, and Y. Wang, IEEE Trans. Electron. Devices **55**, 2960 (2008).
[15]S. Datta, Superlatt. Microstruct. **28**, 253 (2000).
[16]Z. Ren, R. Venugopal, S. Datta, and M. Lundstrom, IEDM **01**, 107 (2001).

[17]Z. Ren, R. Venugopal, S. Goasguen, S. Datta, and M. S. Lundstrom, IEEE Trans. Electron. Devices **50**, 1914 (2003).
[18]M. Bescond, K. Nehari, J. L. Autran, N. Cavassilas, D. Munteanu, and M. Lannoo, IEDM **04**, 617 (2004).
[19]X. Shao and Z. Yu, Solid-State Electron. **49**, 1435 (2005).
[20]E. Dastjerdy, R. Ghayour, and H. Sarvari, Cent. Eur. J. Phys. **9**, 472 (2011).
[21]J. Wang, E. Polizzi, and M. Lundstrom, J. Appl. Phys. **96**, 2192 (2004).
[22]B. Nag Chowdhury and S. Chattopadhyay, Nanosci. Nanotechnol. Lett. **5**, 1087 (2013).
[23]J. Chauhan and J. Guo, Nano Res. **4**, 571 (2011).
[24]D. Nozaki and G. Cuniberti, Nano Res. **2**, 648 (2009).
[25]R. Venugopal, Z. Ren, S. Datta, M. S. Lundstrom, and D. Jovanovic, J. Appl. Phys. **92**, 3730 (2002).
[26]P. S. Damle, A. W. Ghosh, and S. Datta, *Molecular Nanoelectronics* (American Scientific Publishers, California, 2003), p. 115.
[27]M. Miyao, T. Motooka, N. Natsuaki, and T. Tokuyama, Solid State Commun. **37**, 605 (1981).
[28]B. Nag Chowdhury and S. Chattopadhyay, 2nd International Conference on Advanced Nanomaterials and Nanotechnology, Guwahati, India, 2011.
[29]N. Neophytou, A. Paul, M. S. Lundstrom, and G. Klimeck, IEEE Trans. Electron. Devices **55**, 1286 (2008).
[30]S. M. Sze and K. K. Ng, *Physics of Semiconductor Devices* (John Wiley and Sons, Inc. Publication, 2007) p. 314.
[31]M. Luisier and G. Klimeck, Phys. Rev. B **80**, 155430 (2009).
[32]S. Datta, *Quantum Transport: Atom to Transistor* (Cambridge University Press, 2005).